European Heart Journal (2011) **32**, 1251–1259
doi:10.1093/eurheartj/ehq518

In vivo critical fibrous cap thickness for rupture-prone coronary plaques assessed by optical coherence tomography

Taishi Yonetsu[1]*, Tsunekazu Kakuta[1], Tetsumin Lee[1], Kentaro Takahashi[1], Naohiko Kawaguchi[1], Ginga Yamamoto[1], Kenji Koura[1], Keiichi Hishikari[1], Yoshito Iesaka[1], Hideomi Fujiwara[1], and Mitsuaki Isobe[2]

[1]Department of Cardiology, Tsuchiura Kyodo Hospital, 11-7 Manabeshin-machi, Tsuchiura, Ibaraki 300-0053, Japan; and [2]Cardiovascular Medicine, Tokyo Medical and Dental University, Tokyo, Japan

Received 19 May 2010; revised 10 December 2010; accepted 28 December 2010; online publish-ahead-of-print 27 January 2011

Aims The widely accepted threshold of <65 μm for coronary plaque fibrous cap thickness was derived from postmortem studies of ruptured plaques and may not be appropriate for *in vivo* rupture-prone plaques. We investigated the relationship between fibrous cap thickness and plaque rupture using optical coherence tomography (OCT).

Methods and results We studied 266 lesions (103 from patients with acute coronary syndrome and 163 from patients with stable angina) before percutaneous coronary intervention using OCT. Ruptured and non-ruptured lipid-rich plaques were identified and the thinnest and most representative fibrous cap thickness were determined. Cap thickness was reliably measured in 71 ruptured and 111 non-ruptured plaques. From the ruptured plaques, the median thinnest cap thickness was 54 μm (50–60). The median most representative cap thickness was 116 μm (103–136). For non-ruptured plaques, the median thinnest cap thickness was 80 μm (67–104) and 182 μm (156–216) for most representative cap thickness. In 95% of ruptured plaques, the thinnest cap thickness and most representative cap thickness were <80 and <188 μm, respectively. The best cut-offs for predicting rupture were <67 μm (OR: 16.1, CI: 7.5–34.4, $P < 0.001$) for the thinnest cap thickness and <151 μm (OR: 35.6, CI: 15.0–84.3, $P < 0.001$) for most representative cap thickness. These two measures were modestly correlated ($r^2 = 0.39$) and both independently associated with rupture.

Conclusion *In vivo* critical cap thicknesses were <80 μm for the thinnest and <188 μm for most representative fibrous cap thickness. Prospective imaging studies are required to establish the significance of these values.

Keywords Acute coronary syndrome • Atherosclerosis • Plaque • Imaging

Introduction

Coronary plaque rupture is recognized as a major cause of acute coronary syndrome. The characteristics of unstable coronary plaques have been well defined in several pathological studies,[1–4] and fibrous cap thickness is often identified as an important determinant of the degree of plaque instability. Currently, thin-capped fibroatheroma (TCFA) is defined as a plaque with a thin fibrous cap overlying a large lipid pool.[3] Burke *et al.*[4] examined coronary cross sections with more than 50% lumen narrowing and fibrous cap thickness was 23 ± 19 μm in ruptured plaques. They also reported that cap thickness was <65 μm in 95% of ruptured plaques, a value that has since been used as the definition of TCFA. This critical threshold of 65 μm, derived from the fragments of ruptured fibrous caps from 41 cadavers, may not be appropriate for evaluating *in vivo* rupture-prone plaques. Pathologically determined morphometric values might be affected by tissue shrinkage during histological preparations. To circumvent these issues, a method that can directly measure fibrous cap thickness *in vivo* is essential. Optical coherence tomography (OCT) is currently

* Corresponding author. Tel: +81 29 823 3111, Fax: +81 29 823 1160, Email: yonetsu@gmail.com

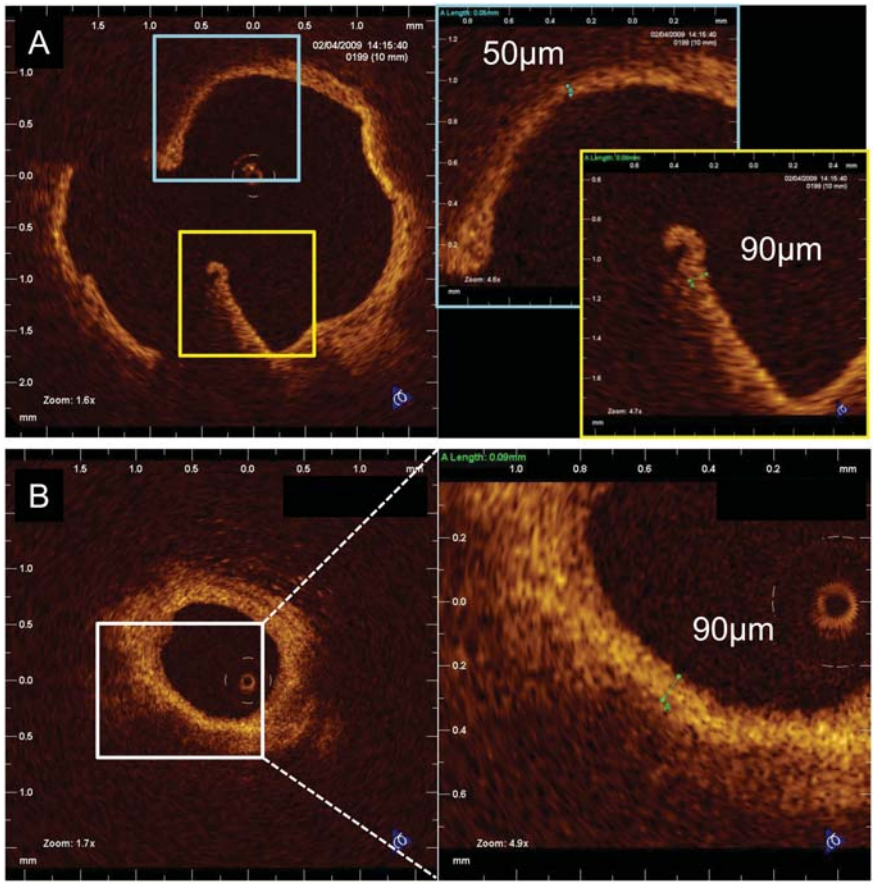

Figure 1 Representative measurements of ruptured (*A*) and non-ruptured (*B*) thinnest cap thickness.

considered the only modality that can directly measure fibrous cap thickness *in vivo*. Cilingiroglu *et al.*[5] demonstrated that OCT can visualize a thin fibrous cap *in vivo*, and Kume *et al.*[6] validated the accuracy of OCT measurements of a fibrous cap compared with histological examinations. Identifying the critical threshold of fibrous cap thickness *in vivo* may contribute to risk stratification of patients and therapeutic targeting. In the present study, we determined the thinnest cap thicknesses in ruptured and non-ruptured lipid-rich plaques using OCT. We also sought to determine the most representative cap thickness in ruptured and non-ruptured plaques and evaluated the thresholds associated with cap rupture. Representative cap thickness was thicker than the thinnest cap thickness and may be a practical target for risk stratifying rupture-prone plaques by imaging modalities if the significance in discriminating non-ruptured lipid-rich plaques from ruptured plaques exists in this measure.

Methods

Study population

Between November 2008 and December 2009, a prospective, non-consecutive series of 266 patients with an identifiable and *de novo* single culprit lesion in a native coronary artery underwent OCT imaging before percutaneous coronary intervention (PCI) with stenting. Of the 266 patients, 103 patients had acute coronary syndrome (ACS) and 163 patients had stable angina pectoris (SAP). Patients were excluded if they had significant left main disease, congestive heart failure, or renal insufficiency with a baseline serum creatinine of $>$1.8 mg/dL (133 μmol/L). In addition, those patients with extremely tortuous vessels or heavy calcification were excluded because of anticipated difficulty in advancing the OCT catheter. Acute myocardial infarction (AMI) was diagnosed in patients with continuous chest pain and abnormal levels of cardiac enzymes (creatinine kinase-MB or troponin-I); of these patients, 39 patients had ST-segment elevation (STEMI) ($>$0.1 mV in two contiguous ECG leads) and 29 patients (NSTEMI) did not. In the current study, STEMI patients treated with stenting within 12 h of symptom onset (mean: 3.9 $\pm$ 1.7 h) were enrolled. In NSTEMI patients, the mean duration from symptom onset to OCT imaging was 1.3 $\pm$ 2.0 days. Platelet glycoprotein IIb/IIIa receptor inhibitors were not used because they are not available in Japan. In AMI patients, manual aspiration thrombectomy was performed at operator's discretion and patients with a Thrombolysis in Myocardial Infarction (TIMI) flow grade $\leq$2 after thrombectomy were excluded from the study. Unstable angina pectoris (UAP) was defined as a progressive crescendo ECG pattern or angina at rest, without an increase of troponin-I. SAP was defined as no change in frequency, duration, or intensity of anginal symptoms within the 6 weeks preceding the intervention. Infarct-related or target lesions were identified by the combination of left ventricular wall motion abnormalities, ECG findings, angiographic

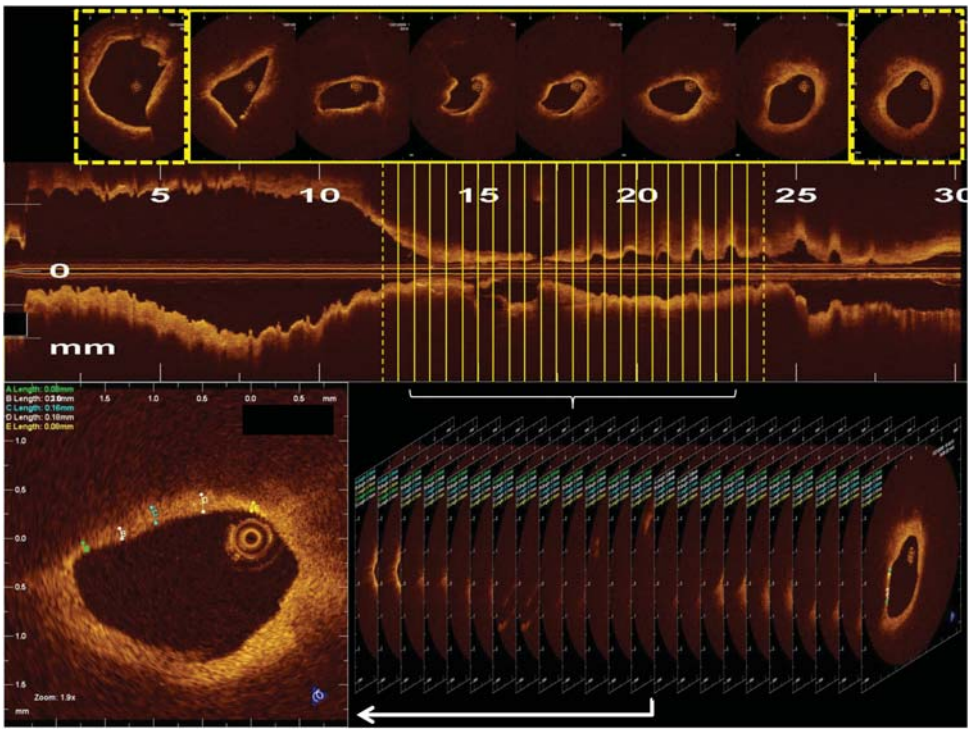

Figure 2 Exemplification of most representative cap thickness of a ruptured lipid-rich plaque. Cap thickness was measured at five randomly selected sites at the cross-sectional image and the average value was calculated. The measurements were performed at every 10th image (0.5 mm interval) throughout the lipid-rich plaque and the mean value was obtained as most representative cap thickness.

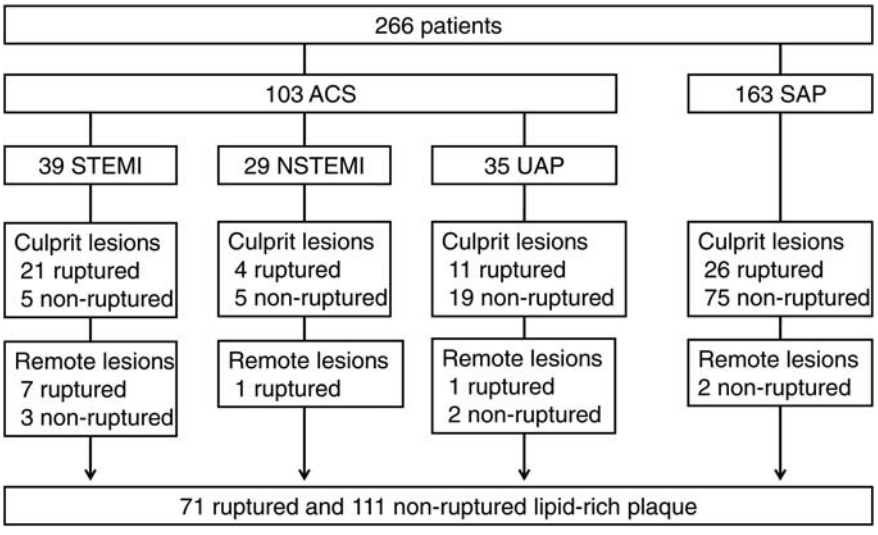

Figure 3 Among 266 culprit arteries in 266 patients, optical coherence tomography identified 71 ruptured and 111 non-ruptured lipid-rich plaques in which reliable measurements of fibrous cap thickness could be performed. Lesions with large thrombus burden, suspected erosion, Thrombolysis in Myocardial Infarction flow grade ≤ 2 after thrombectomy, and lesions which required balloon predilatation for optical coherence tomography imaging were excluded.

lesion morphology, and scintigraphic defects. The study protocol was approved by the institutional review board, and all patients provided written informed consent prior to PCI.

Angiographic analysis

Quantitative coronary angiography was performed using a CMS-MEDIS system (Medis Medical Imaging Systems, Leiden, The

Table 1 Patient characteristics

	Ruptured ($n = 71$)	Non-ruptured ($n = 111$)	*P*-value
Age, years	65.3 ± 11.8	66.1 ± 11.0	0.66
Male gender, *n* (%)	62 (87.3)	89 (80.2)	0.23
CRP, mg/dL	0.0 (0.0–0.35)	0.0 (0.0–0.24)	0.38
WBC, count/μL	7690 (5880–9310)	6210 (4960–7450)	<0.001
Total cholesterol, mg/dL	194.5 ± 40.3	194.4 ± 38.3	0.98
LDL-cholesterol, mg/dL	115 (98–145)	114 (94–142)	0.80
HDL-cholesterol, mg/dL	43 (37–48)	42 (34–53)	0.73
TG, mg/dL	128 (85–181)	136 (95–180)	0.77
HbA1c, %	5.5 (5.1–7.4)	5.7 (5.3–6.6)	0.94
Creatinine, mg/dL	0.81 (0.70–1.10)	0.80 (0.68–0.96)	0.38
eGFR, mL/min	68.5 ± 30.4	72.0 ± 21.5	0.40
Diabetes, *n* (%)	27 (38.0)	43 (38.7)	1.000
Hypertension, *n* (%)	49 (69.0)	85 (76.6)	0.30
Dyslipidemia, *n* (%)	40 (56.3)	66 (59.5)	0.76
Current smoking, *n* (%)	35 (49.3)	46 (41.4)	0.36
Statin use, *n* (%)	27 (38.0)	57 (51.4)	0.094
Clinical presentation, *n* (%)			
STEMI	28 (39.4)	8 (7.2)	<0.001
NSTEMI	5 (7.0)	5 (4.5)	0.52
UAP	12 (16.9)	21 (18.9)	0.84
SAP	26 (36.6)	77 (69.4)	<0.001

CRP, C reactive protein; WBC, white blood cell; TG, triglyceride; eGFR, estimated glomerular filtration rate; LDL, low density lipoprotein; HDL, high density lipoprotein.

Table 2 Angiographic findings

	Ruptured ($n = 71$)	Non-ruptured ($n = 111$)	*P*-value
Lesion location, *n* (%)			0.025
RCA	37 (52.1)	35 (31.5)	
LAD	23 (32.4)	54 (48.6)	
Cx	11 (15.5)	22 (19.8)	
QCA data			
MLD, mm	0.81 (0.30–1.12)	0.97 (0.69–1.18)	0.008
RD, mm	3.01 (2.66–3.34)	2.68 (2.45–3.03)	<0.001
DS, %	72.2 (59.9–88.1)	64.3 (56.4–74.3)	<0.001
Lesion length, mm	13.9 (11.2–18.4)	12.7 (9.9–18.4)	0.27

RCA, right coronary artery; LAD, left anterior descending artery; Cx, circumflex artery; MLD, minimum lumen diameter; RD, reference diameter; DS, diameter stenosis.

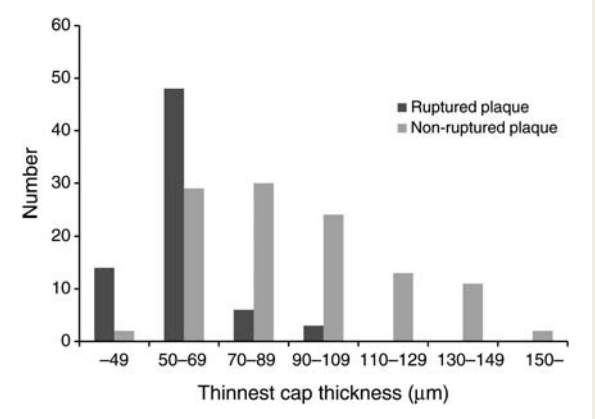

Figure 4 Number of plaques according to the thinnest cap thickness and rupture. Bar graph showing the distribution of ruptured and non-ruptured plaques according to the thinnest cap thickness.

Netherlands). The length, minimum lumen diameter, and reference lumen diameter of the culprit lesions were measured. Coronary flow was assessed according to TIMI flow grade.[7]

OCT image acquisition

Aspirin (200 mg), clopidogrel (300 mg for ACS, 75 mg for SAP), and intravenous heparin (100 U/kg) were administered before coronary catheterization. OCT imaging was performed before any intervention and after intracoronary administration of nitroglycerin (0.2 mg) in patients with ACS, with a TIMI flow grade of 3, or patients with SAP. In patients with AMI, aspiration thrombectomy was performed using an aspiration catheter (Eliminate, TERUMO, Tokyo, Japan) prior to OCT imaging if there was an angiographically suspected thrombus or TIMI flow grade ≤2. The OCT system used in this study (LightLab Imaging, Inc., Westford, MA, USA) has been described previously.[8,9] The axial and lateral resolutions based on the manufacturer specifications are 15–20 and 20–40 μm, respectively. An OCT balloon catheter (Helios; Goodman, Nagoya, Japan) was advanced to the tip of the guiding catheter over the OCT imaging wire. Then the OCT imaging wire was advanced to a position distal in the culprit coronary artery and the OCT balloon catheter advanced over the imaging wire proximal to the lesion. If the lesion could not be crossed by the imaging wire, we first advanced a conventional coronary guidewire (0.014 inches) through the lesion before replacing it with the OCT imaging wire over the balloon catheter. Lesions in which predilatation using a balloon was required to cross the OCT imaging wire were excluded from the study. The lesion and segments distal and proximal to the lesion were visualized using an automated pullback system at 1.0 mm/s. During image acquisition, coronary blood flow was replaced by a continuous infusion of Ringer's lactate from the distal tip of the balloon catheter. The highly compliant occlusion balloon remained inflated proximal to the lesion at 0.5–0.7 atm. When a lesion was located close (<1 cm) to the ostium of the coronary arteries, we used a continuous-flushing, non-occlusive technique for OCT imaging.[10] To remove blood from the vessel without occlusion, we infused commercially available dextran-40 and lactated Ringer solution

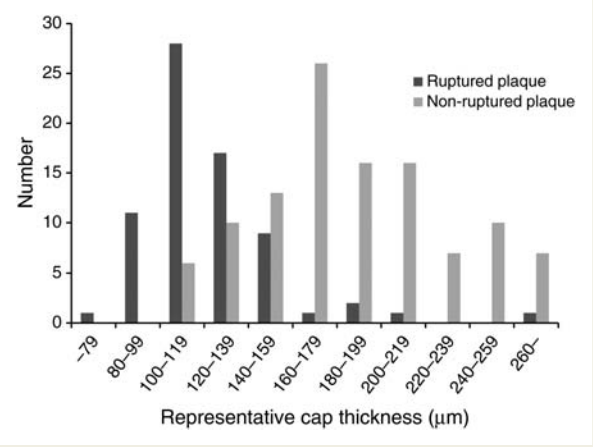

Figure 5 Number of plaques according to representative cap thickness and rupture. Bar graph showing the distribution of ruptured and non-ruptured plaques according to representative cap thickness.

Table 3 Threshold values obtained in the present study

	Thinnest cap thickness	Most representative cap thickness
Median value		
Ruptured plaque ($n = 71$), μm	54 (50–60)	116 (103–136)
Non-ruptured plaque ($n = 111$), μm	80 (67–104)	182 (156–216)
Value in 95% of ruptured plaque, μm	<80	<188
The best cut-off value in ROC analysis, μm	<67	<151

(Low Molecular Dextran L, Otsuka Pharmaceutical Factory, Tokushima, Japan) directly from the guiding catheter at 3.0–4.0 mL/s using a power injector (Angimat Illumena, Liebel-Flarsheim, Cincinnati, OH, USA). The entire length of the culprit lesion was cross sectionally imaged by OCT, with repeated pullback procedures at 20 frames/s.

Image analysis

OCT images were digitalized and analysed using proprietary software (LightLab Imaging, Inc.) according to the principals of OCT imaging described elsewhere.[9,11–13] All OCT images were analysed by two independent investigators (T.Y. and T.K.) who were blinded to the clinical presentations. When there was discord between the observers, a consensus reading was obtained. Lesions with the images showing significant signal attenuation or a large thrombus burden precluding satisfactory evaluation and reliable morphological measurement were excluded from the analysis. Analysis of contiguous cross sections was performed in all analysable cross-sectional images (50 μm interval). Lipid content was semi-quantified due to the number of involved quadrants on the cross-sectional OCT image. A fibrous cap was identified as a signal-rich homogenous region overlying a lipid core, which was characterized by a diffusely bordered, signal-poor region on the OCT image. A lipid-rich plaque was defined as a plaque with a fibrous cap thickness of <400 μm over OCT-derived lipid and extending for more than one quadrant of the vessel circumference. The presence of lipid-rich plaques, with or without rupture, was documented. Fibrous cap disruption was identified by the presence of fibrous cap discontinuity and a cavity formation within the plaque. When fibrous cap disruption was present in a lipid-rich plaque, it was considered a ruptured lipid-rich plaque. Currently, fibrous cap erosion is difficult to prospectively identify because it does not have a typical and definitive morphological signature that can be detected by OCT. Therefore, plaques with suspected plaque erosion were excluded from the analysis. The lipid-rich plaque had to be visible in more than 10 consecutive cross-sectional images. A lipid-rich plaque, separated by a length of coronary artery, with fibrous or fibrocalcific plaque containing smooth lumen contours and no cavity formation, was considered to represent a different plaque and included in the analysis. The thinnest fibrous cap thickness was defined as the distance from the arterial lumen to the inner border of the lipid pool where the fibrous cap thickness is considered minimal in non-ruptured lipid-rich plaques. For ruptured plaques, the thinnest cap thickness was measured both at non-ruptured portion without communication between the lipid core and the lumen and at the thinnest part of the remnant of the disrupted fibrous cap. The thinnest cap thicknesses for each image were measured at two different times, and the average value was obtained. Minimum values, among the average values from each OCT image, were used for the analysis. For most representative cap thickness, cap thickness was measured at five randomly selected sites at the cross-sectional image and the average value was calculated. The measurements were performed at every 10th image throughout the plaque (0.5 mm interval) and the mean value was obtained as most representative cap thickness. Cap thicknesses were compared between ruptured and non-ruptured groups. Representative measurements of the thinnest and most representative fibrous cap thickness are shown in *Figures 1* and *2*. Inter- and intra-observer variabilities were assessed by evaluating measurements by the two independent readers and by evaluating all images by the same reader after an interval of at least 1 week, respectively.

Statistical analysis

SPSS, version 14.0 (SPSS Inc., Chicago, IL) was used for all analyses. Categorical data were expressed as absolute frequencies and percentages and were compared using the χ^2 or Fisher exact test, as appropriate. Continuous variables were expressed as either mean ± SD for normally distributed variables or median (25th to 75th percentiles) for non-normally distributed variables and compared using either unpaired Student's *t*-test or Mann–Whitney U-tests, respectively. Receiver operating characteristics (ROC) analysis was used to determine the best cut-off cap thickness values for discriminating between ruptured and non-ruptured plaques. The relationship between plaque rupture (dependent variable), cap thickness, and other potential confounders was assessed using stratified multivariable logistic regression analysis (stepwise forward method) to assess whether quartile categories (transformed into categories for decreasing values) of the measures of cap thickness were associated with plaque rupture. Significant variables on univariate analyses ($P < 0.2$) were included in the multivariable model. Inter- and intra-observer agreement for identification of lipid-rich plaques and the presence of plaque rupture was evaluated by κ statistics of concordance. The intra- and inter-observer variabilities for cap thickness values were evaluated by linear regression

Table 4 Cut-off values of cap thickness for detection of ruptured plaques

	Thinnest cap thickness <67 μm	Representative cap thickness <151 μm	Thinnest cap thickness <67 μm and representative cap thickness <151 μm
Sensitivity, % (95% CI)	83.1 (72.3–91.0)	87.3 (80.0–92.5)	76.1 (68.5–81.8)
Specificity, % (95% CI)	76.6 (67.6–84.1)	83.8 (79.1–87.1)	89.2 (84.4–92.9)
Positive predictive value, % (95% CI)	69.4 (58.5–79.0)	77.5 (71.0–82.1)	81.8 (73.7–88.0)
Negative predictive value, % (95% CI)	87.6 (79.4–93.4)	91.2 (86.1–94.8)	85.3 (80.7–88.9)
Correct classification rate, % (95% CI)	79.1 (72.9–83.9)	85.2 (79.5–89.2)	84.1 (78.2–88.6)

analysis and the absolute mean difference between two measurements. A $P < 0.05$ was considered statistically significant.

Results

Mean examined length by OCT in each patient was 42 ± 11 mm. In all 266 examined vessels, OCT identified 71 (STEMI, 28; NSTEMI, 5; UAP, 12; SAP, 26) ruptured and 111 (STEMI, 8; NSTEMI, 5; UAP, 21; SAP, 77) non-ruptured lipid-rich plaques in which fibrous cap thickness could be reliably measured. A summary of the plaque identification and diagnosis is shown in *Figure 3*. Among them, 62 ruptured plaques were detected at the culprit lesions and 9 remote ruptured plaques were found. For non-ruptured lipid-rich plaques, 104 were observed in the culprit lesions and 7 were remote. Large thrombus burden precluding reliable measurements of cap thickness was the major cause of exclusion in patients with ACS.

Patients characteristics and angiographic findings

Baseline clinical characteristics and angiographic findings are summarized in *Tables 1* and *2*. There were no statistically significant differences in terms of age, gender, or other important coronary risk factors between the two groups. White blood cell count at admission was significantly higher in patients with ruptured plaques than in patients without.

OCT findings

Using OCT, culprit sites were successfully observed in all patients without any serious procedural complications. Flushing technique was applied for 17 patients (6.4%). In these patients, 4 ruptured and 6 non-ruptured lipid-rich plaques were analysed. *Figures 4* and *5* show the numbers of ruptured and non-ruptured plaques according to the thinnest and representative cap thickness. *Table 3* listed the threshold values obtained in the present study. In ruptured plaques, the median thinnest cap thickness was 54 μm (IQR: 50–60 μm). The thinnest cap thickness was obtained at the portion of ruptured cap fragments in only 15 of 71 ruptured plaques (21.1%). In the remaining 56 ruptured plaques, the thinnest cap thickness was obtained at the undisrupted portion of the fibrous cap. The median thinnest cap thickness of non-ruptured plaques was 80 μm (67–104 μm) and significantly thicker than

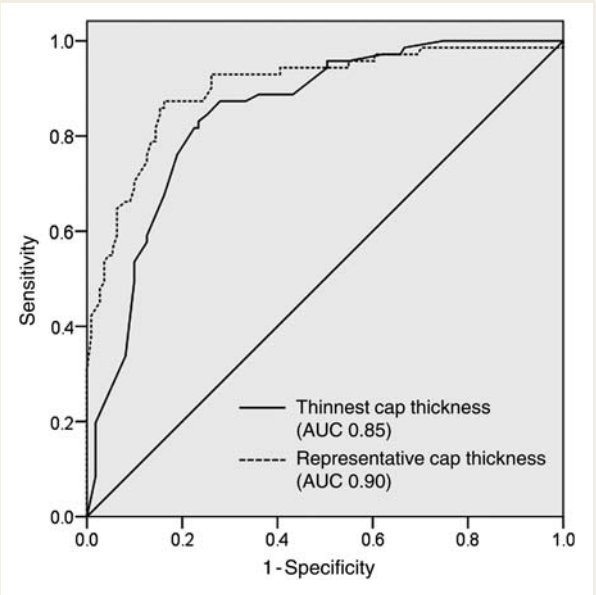

Figure 6 Receiver operating characteristic curves for measurements of fibrous cap thickness for prediction of fibrous cap rupture. AUC, area under the curve.

ruptured plaques ($P < 0.001$). The thinnest cap thickness was <80 μm in 95% of ruptured lipid-rich plaques. This value is comparable to the threshold of <65 μm, derived from the previously mentioned pathological studies,[3,4] although cap thickness was examined not only at the ruptured cap remnants but in the entire plaque including non-ruptured portion of ruptured plaques in the present study. The median most representative cap thickness for ruptured plaques was 116 μm (103–136 μm) vs. 182 μm (156–216 μm) for non-ruptured plaques ($P = 0.01$). In 95% of ruptured plaques, most representative cap thickness was <188 μm. There was no significant difference in both measures in ruptured plaques between ACS and SAP (the thinnest cap thickness: 52 μm (50–59) vs. 60 μm (52–64), $P = 0.06$; representative cap thickness: 122 μm (103–136) vs. 111 μm (103–140), $P = 0.54$, respectively). In ROC analysis, the best cap thickness values for predicting rupture were a thinnest cap thickness of <67 μm and a representative cap thickness of <151 μm (*Table 4*). Both

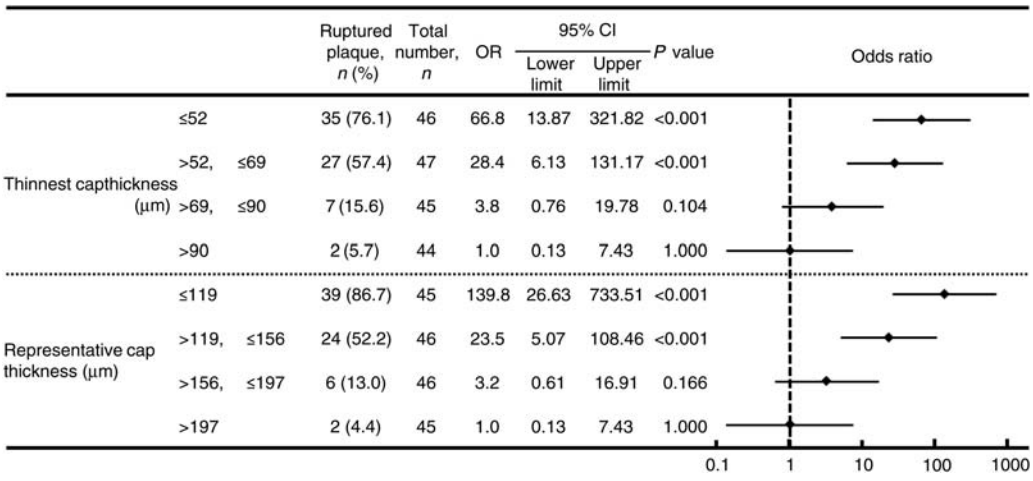

Figure 7 Odds ratios for the presence of rupture according to quartiles of cap thickness values for the thinnest cap thickness and representative cap thickness. Values were assessed in comparison with highest thickness quartile.

Table 5 Univariate and multivariable logistic regression analyses

	Univariate logistic regression			Multivariable logistic regression		
	OR	**95% CI**	***P*-value**	**OR**	**95% CI**	***P*-value**
WBC	1.0003	1.0002–1.0004	<0.001	1.0003	1.0001–1.0005	0.008
ACS	3.92	2.09–7.35	<0.001			
RCA	2.36	1.28–4.37	0.006			
RD	3.43	1.79–6.58	<0.001	4.22	1.53–11.6	0.005
Statin use	0.58	0.32–1.07	0.08			
Thinnest cap thickness	4.22	2.79–6.40	<0.001	1.88	1.12–3.14	0.016
Representative cap thickness	5.86	3.60–9.55	<0.001	4.02	2.32–7.00	<0.001

WBC, white blood cell; ACS, acute coronary syndrome; RCA, right coronary artery; RD, reference diameter

measures provide highly significant discriminating performance for plaque rupture (*Figure 6*). Thinnest cap thickness and representative cap thickness were modestly correlated ($r^2 = 0.39$, $P < 0.001$). When all lipid-rich plaques were divided into quartiles by corresponding cap thickness values, there was an inverse relationship between the two measures of cap thickness and cap rupture (*Figure 7*). Multivariable logistic regression analysis revealed that the thinnest and most representative cap thicknesses, white blood cell count, and reference diameter were independently associated with cap rupture (*Table 5*).

Intra- and Inter-observer variability

Intra-observer variability yielded acceptable concordance for exclusion or inclusion on the basis of image quality ($\kappa = 0.91$), the presence of lipid-rich plaques ($\kappa = 0.86$), and plaque rupture ($\kappa = 0.89$). Inter-observer variability showed slightly lower concordance for exclusion or inclusion into the analysis ($\kappa = 0.82$), the presence of lipid-rich plaques ($\kappa = 0.78$), and plaque rupture ($\kappa = 0.80$). Mean inter-observer differences in the thinnest cap and representative cap thicknesses were 5.3 ± 9.7 and 11.2 ± 8.6 μm, respectively. Mean intra-observer differences in thinnest and representative cap thicknesses were 3.8 ± 6.7 and 9.4 ± 7.9 μm, respectively. Intra- and inter-observer correlation coefficients for measurements of representative cap thickness were 0.93 and 0.87, respectively.

Discussion

This is the first *in vivo* OCT study showing that the critical thinnest fibrous cap thickness of ruptured plaques is 80 μm and that the most representative fibrous cap thickness determined by multiple measurements is independently and significantly associated with plaque rupture.

The current paradigm postulates a particular plaque morphology for rupture-prone plaques, including large lipid cores, thin fibrous cap, and assessment of inflammation.[3] While OCT cannot quantify

lipid content, its high resolution allows us to visualize and quantify the thin fibrous cap.[9,12] Virmani *et al.*[3,4] reported that, in ruptured plaques from a series of 41 cadavers who died suddenly, the minimum cap thickness at the point of rupture was 23 μm, and 95% of the disrupted caps were <65 μm. This cap thickness value from postmortem studies has been widely used as the definition of *in vivo* non-ruptured TCFA. Acknowledging the lack of prospective studies to define rupture-prone plaques, the consensus opinion is that the majority of acute coronary events originate from plaque rupture of TCFA,[3,9,12,14–17] and the importance of fibrous cap thickness has been consistently demonstrated in a number of studies.[3,18] The present *in vivo* OCT examination found that 95% of ruptured plaques were <80 μm. This discrepancy between *in vivo* and *ex vivo* data may be explained by anisotropic tissue shrinkage during pathological preparations,[19] difference in study population, or methodology of determining fibrous cap thickness. Previous studies measured the thinnest cap thickness at the ruptured cap fragments.[3,4,9] In the current study, the thinnest portion of the ruptured plaques was observed at a non-ruptured portion of the cap in 78.9% (56/71). This finding indicates that the disrupted portion of the cap may not necessarily represent the thinnest cap thickness. Although we do not really know what the critical thickness of the fibrous cap is at the site of rupture and at the time of rupture, we propose that fibrous cap thickness of <80 μm may be used as an alternative threshold of critical threshold of cap thickness *in vivo*.

The median most representative cap thickness of ruptured and non-ruptured plaques were 116 and 182 μm, respectively ($P < 0.001$). These values were significantly greater than the thinnest cap thicknesses. These findings suggest that cap thinning may occur diffusely, rather than focally, in the entire fibrous cap of lipid-rich plaque. In the present study, most representative cap thickness was obtained by multiple measurements with an interval of 0.5 mm. However, these measurements are susceptible to subjectivity, and fibrous cap thickness values including the thinnest and the representative cap thickness are largely influenced by the quantitative methods and should be interpreted with caution.

Both inflammatory markers of WBC and C reactive protein have been implicated as associated or causal factors in the pathogenesis of atherosclerotic coronary plaques.[20] In the present study, WBC count was associated with ruptured plaques, whereas no relationship was found between CRP and ruptured plaques. This finding may be explained by the heterogeneous study cohort including STEMI, NSTEMI, UAP, and SAP between ruptured and non-ruptured groups in the present study. Blood sampling was performed once at the time of admission and WBC count might have already increased before CRP elevation in the ruptured group irrespective of the baseline inflammatory status because the majority of STEMI patients were in the ruptured group.

In multivariable analysis, the thinnest and representative cap thickness were independent predictors of plaque rupture. From these results, representative cap thickness of <188 μm (value in 95% of ruptured plaques) can be used for risk-stratifying high-risk, rupture-prone plaques. Our findings may provide estimates for the required resolution of imaging modalities for future natural history studies of atherosclerotic plaques. Future non-invasive coronary imaging may make detection of a representative cap thickness of 188 μm possible, likely earlier than imaging that will allow for the resolution of 80 μm for the critical thinnest cap thickness. Future prospective imaging studies using the thresholds suggested in the current study are required to establish whether these values predict plaque rupture or clinical events.

Limitation

A number of limitations in the present study should be appreciated. First, a prospective, but non-consecutive series, of subjects who met the eligibility criteria and consented to the study were enrolled. Excluding patients or lesions may have resulted in a selection bias. However, enrollment criteria are common in the majority of the studies that require invasive imaging and are necessary for subject safety. Second, lesions with large thrombus burdens were excluded because no reliable OCT analysis for cap thickness could be performed. Exclusion of these lesions, especially from ACS patients, may have caused additional selection bias, although this limitation is inevitable when using the current OCT system *in vivo*. Third, we cannot exclude the possibility that the guiding catheter manipulation, contrast injection, guidewire crossing if required, or OCT imaging wire itself may have altered plaque morphology. However, in the present study, we excluded ambiguous plaque ruptures, such as plaques with suspected cap erosion or small fissures in size and length for reliable cap thickness measurements. Fourth, flushing technique was applied for 17 lesions (6.4%) without proximal occlusion and might have affected cap thickness measurements and image quality. Fifth, the lack of a pre-specified or automated selection of the sites of measurements within the plaque and software-based automated cap thickness measurements make the present method less objective and prone to variability and individual interpretation. In addition, we did not evaluate the relationship between plaque rupture and clinical presentation. Asymptomatic plaque rupture is not uncommon, and multiple factors including cap thickness may be involved in the process of rupture-induced coronary thrombosis. TCFA and ruptured plaque may arise or heal quickly,[21] and time course, or definitive cap thickness at the time of rupture, cannot be determined by studies that take only one time point into account. Prospective studies of *in vivo* serial imaging should be performed to determine the predictive value for rupture and frequency of rupture-induced cardiac events.

Conclusion

The thinnest cap thickness was obtained at the undisrupted portion of the fibrous cap in the majority of ruptured plaques (78.9%). A thinnest cap thickness of <80 μm is the critical cap thickness for plaque rupture in living patients. A representative cap thickness of <188 μm obtained from multiple measurements may be used as an alternative threshold of critical fibrous cap thickness *in vivo*. Future prospective *in vivo* studies are required to validate whether these cut-off values predict plaque rupture or clinical events or serve as a therapeutic target for both patients of coronary artery disease and asymptomatic individuals.

Conflict of interest: none declared.

References

1. Fuster V, Moreno PR, Fayad ZA, Corti R, Badimon JJ. Atherothrombosis and high-risk plaque: part I: evolving concepts. *J Am Coll Cardiol* 2005;**46**:937–954.
2. Virmani R, Burke AP, Farb A, Kolodgie FD. Pathology of the vulnerable plaque. *J Am Coll Cardiol* 2006;**47**(8 Suppl.):C13–C18.
3. Virmani R, Kolodgie FD, Burke AP, Farb A, Schwartz SM. Lessons from sudden coronary death: a comprehensive morphological classification scheme for atherosclerotic lesions. *Arterioscler Thromb Vasc Biol* 2000;**20**:1262–1275.
4. Burke AP, Farb A, Malcom GT, Liang YH, Smialek J, Virmani R. Coronary risk factors and plaque morphology in men with coronary disease who died suddenly. *N Engl J Med* 1997;**336**:1276–1282.
5. Cilingiroglu M, Oh JH, Sugunan B, Kemp NJ, Kim J, Lee S, Zaatari HN, Escobedo D, Thomsen S, Milner TE, Feldman MD. Detection of vulnerable plaque in a murine model of atherosclerosis with optical coherence tomography. *Catheter Cardiovasc Interv* 2006;**67**:915–923.
6. Kume T, Akasaka T, Kawamoto T, Okura H, Watanabe N, Toyota E, Neishi Y, Sukmawan R, Sadahira Y, Yoshida K. Measurement of the thickness of the fibrous cap by optical coherence tomography. *Am Heart J* 2006;**152**:755, e751–e754.
7. The Thrombolysis in Myocardial Infarction (TIMI) Trial. Phase I findings. TIMI Study Group. *N Engl J Med* 1985;**312**:932–936.
8. Tanigawa J, Barlis P, Di Mario C. Intravascular optical coherence tomography: optimisation of image acquisition and quantitative assessment of stent strut apposition. *EuroIntervention* 2007;**3**:128–136.
9. Kubo T, Imanishi T, Takarada S, Kuroi A, Ueno S, Yamano T, Tanimoto T, Matsuo Y, Masho T, Kitabata H, Tsuda K, Tomobuchi Y, Akasaka T. Assessment of culprit lesion morphology in acute myocardial infarction: ability of optical coherence tomography compared with intravascular ultrasound and coronary angioscopy. *J Am Coll Cardiol* 2007;**50**:933–939.
10. Prati F, Cera M, Ramazzotti V, Imola F, Giudice R, Albertucci M. Safety and feasibility of a new non-occlusive technique for facilitated intracoronary optical coherence tomography (OCT) acquisition in various clinical and anatomical scenarios. *EuroIntervention* 2007;**3**:365–370.
11. Jang IK, Tearney GJ, MacNeill B, Takano M, Moselewski F, Iftima N, Shishkov M, Houser S, Aretz HT, Halpern EF, Bouma BE. In vivo characterization of coronary atherosclerotic plaque by use of optical coherence tomography. *Circulation* 2005; **111**:1551–1555.
12. Yabushita H, Bouma BE, Houser SL, Aretz HT, Jang IK, Schlendorf KH, Kauffman CR, Shishkov M, Kang DH, Halpern EF, Tearney GJ. Characterization of human atherosclerosis by optical coherence tomography. *Circulation* 2002; **106**:1640–1645.
13. Prati F, Regar E, Mintz GS, Arbustini E, Di Mario C, Jang IK, Akasaka T, Costa M, Guagliumi G, Grube E, Ozaki Y, Pinto F, Serruys PW. Expert review document on methodology, terminology, and clinical applications of optical coherence tomography: physical principles, methodology of image acquisition, and clinical application for assessment of coronary arteries and atherosclerosis. *Eur Heart J* 2010; **31**:401–415.
14. Tearney GJ, Yabushita H, Houser SL, Aretz HT, Jang IK, Schlendorf KH, Kauffman CR, Shishkov M, Halpern EF, Bouma BE. Quantification of macrophage content in atherosclerotic plaques by optical coherence tomography. *Circulation* 2003;**107**:113–119.
15. Davies MJ, Thomas AC. Plaque fissuring—the cause of acute myocardial infarction, sudden ischaemic death, and crescendo angina. *Br Heart J* 1985;**53**:363–373.
16. Fuster V. Elucidation of the role of plaque instability and rupture in acute coronary events. *Am J Cardiol* 1995;**76**:24C–33C.
17. Falk E, Shah PK, Fuster V. Coronary plaque disruption. *Circulation* 1995;**92**: 657–671.
18. Kolodgie FD, Burke AP, Farb A, Gold HK, Yuan J, Narula J, Finn AV, Virmani R. The thin-cap fibroatheroma: a type of vulnerable plaque: the major precursor lesion to acute coronary syndromes. *Curr Opin Cardiol* 2001;**16**:285–292.
19. Lee RM. A critical appraisal of the effects of fixation, dehydration and embedding of cell volume. In: Revel JP, Barnard T, Haggis GH, eds. *Scanning Electron Microscopy*. Chicago, IL: AMF O'Hare; 1984. p61–70.
20. Margolis KL, Manson JE, Greenland P, Rodabough RJ, Bray PF, Safford M, Grimm RH Jr, Howard BV, Assaf AR, Prentice R, for the Women's Health Initiative Research Group. Leukocyte count as a predictor of cardiovascular events and mortality in postmenopausal women: the Women's Health Initiative Observational Study. *Arch Intern Med* 2005;**165**:500–508.
21. Schoenhagen P, Nissen SE. Coronary atherosclerotic disease burden: an emerging endpoint in progression/regression studies using intravascular ultrasound. *Curr Drug Targets Cardiovasc Haematol Disord* 2003;**3**:218–226.